XIX IMEKO World Congress
Fundamental and Applied Metrology
September 6−11, 2009, Lisbon, Portugal

SPECTRAL REFLECTANCES OF LOG ENDS FOR CAMERA BASED ANNUAL RING WIDTH MEASURMENTS

Marjanen Kalle [1], *Ojala Petteri* [2] *Mäkinen Martti* [3]

[1] Tampere University of Technology, Department of Automation Science and Engineering, Tampere, Finland, kalle.marjanen@tut.fi
[2] Tampere University of Technology, Department of Automation Science and Engineering, Tampere, Finland, petteri.ojala@tut.fi
[3] University of Joensuu, Department of Physics and Mathematics, Joensuu, Finland, martti.makinen@joensuu.fi

Abstract − The wood quality measurement methods are of increasing importance in the wood industry. One of the main goals of the wood industry is to produce new high quality products with higher marketing value. The wood strength and stiffness are significant factors considering wooden products. These factors are related to the wood species, to the number and type of knots and to the mean annual ring width and its deviation to name a few. The logs can be measured and imaged in the forest machinery and thus the measurement based decisions can be made as early as possible on the production chain. This paper focuses on an aspect of the annual ring width estimation from the images taken in forest machinery. The focus is on the spectral reflectance of the log ends for optimal annual ring visibility. The average spectral reflectance of the log end does not indicate how well the annual rings are visible. Therefore a more sophisticated analysis of the annual ring visibility is performed to four tree species based on the two-dimensional spatial spectral analysis.

Keywords: spectral reflectance of the tree, annual ring, image based measurement

1. INTRODUCTION

The search for new and high quality products in the wood industry is of increasing importance. The need for the high quality products implies to a better design and control of the logistics and production chain. The quality measurements of the raw material are important when this point of view is considered. There exist two aims for the development of quality measurements. The first is to provide new, easier and more accurate measures of raw materials quality. The second is to move the measurements and thus the measurement based decision making earlier on the production chain.

The first aim implies to development, testing and implementation of new measurement methods. One of these new methods is the image based measurement of the annual ring width. The second aim implies to harvester or forest machinery implemented outdoor measurements. The outdoor measurements have some significant challenges of their own. These challenges are caused by the environment that is somewhat hostile towards any measurements. The humidity and rain and dust combined with the mechanical vibrations set limitations to hardware used. The change of the illumination during the day [3] combined with the mechanical vibrations degrades the image quality [9] unless special care is taken.

The camera based measurements provide methods for non-intrusive quality analysis. The images taken from logs are a rich source of information about the quality. These images can be used directly by the human observer or by the automatic measurement and classification systems. The automatic image based measurement systems can contain three-dimensional measurements such as close range photogrammetric measurements [7], structural light based systems [8] or combination of both methods in harvesters [6]. Some measurements might contain the measurement of rot amount or strength and stiffness estimation of the log based on the variation of annual ring width [9].

The spectral properties of several plants, trees and leafs [15] are studied widely in the scientific community. The remote sensed aerial or orbital spectral images [16] are often used for the classifying of the tree species [17] or for the classifying of different vegetation types or ages [14]. This paper focuses on the spectral properties of the annual rings. The aim is to find out which wavelengths should be used for the annual ring width measurements for best performance of the measurement system. Our previous assumption is that the annual rings are best visible from 450 to 500 nm for the spruce. This is not probably the case for other trees. Therefore spectral reflectances are measured for three tree species that are the spruce (*Picea abies*), the pine (*Pinus sylvestris*) and the western yellow pine (*Pinus ponderosa*). Visibility functions for the annual rings are provided for wavelengths from 400 nm to 1000 nm.

This paper is organized as follows. The basic properties of illumination, reflection and camera are shortly presented in chapter 2. The reflectance measurement system and method is presented on the chapter 3. The method for visibility curve computation based on the two-dimensional

ISBN 978-963-88410-0-1

spectrum is presented on chapter 4. The resulting mean reflectance curves and visibility curves for the four selected wood species are given in chapter 5. Finally, the conclusions are drawn from the visibility curve measurements.

2. ILLUMINATION, REFLECTION AND CAMERA

The spectral properties of illumination, reflection of target and quantum efficiency of an image sensor are equally important factors in imaging. The success of the image based measurement system is based on these factors. If one factor is limited, others should change in order to keep result the same [1]. A simplified model for the value of the gray scale digital image pixel is of a form

$$P = k\int_{\lambda_1}^{\lambda_2} S(\lambda)\rho(\lambda)\eta(\lambda)d\lambda\,, \qquad (1)$$

where P is the measured grey value, k is a scaling factor, λ_1 and λ_2 are the lower and upper limits of the light wavelength band used, $S(\lambda)$ is the spectral energy distribution of the light source, $\rho(\lambda)$ spectral reflectance of the target and $\eta(\lambda)$ is the quantum efficiency of camera sensor.

The spectral properties of the light source can be optimized for the outdoor use. In [3] LED illumination and a camera filter with a matching pass band are used to observe annual rings. Use of matched LED illumination-camera filter combination achieved imaging that is independent of the ambient light (natural light, lights of the forest machinery etc.). The spectral properties of the light (and the optical filters) should be matched to the annual rings spectral properties also to provide a maximal performance. Therefore the measurement of the annual ring visibility is needed.

The fundamental components of wood (lignin, cellulose, water) have an uneven spectral response [2] and thus some wavelengths are more effective in the observation of specific features involving aforementioned components than others. The spring wood and the summer wood differ in their structures and are visually different thus are enabling the computation of annual ring widths.

The camera quantum efficiency is one of the three basis factors of imaging. The quantum efficiency is the number of independent electrons produced per photon [12] and is always smaller than one. The common day light digital cameras having silicon based sensors tend to be sensitive to radiation from approximately 350 nm to 1150 nm [12]. The effect of the camera quantum efficiency is not discussed in this paper although it is important factor on the imaging system design.

3. SPECTRAL REFLECTANCE MEASUREMENT

Studied tree species are the spruce (*Picea abies*), pine (*Pinus sylvestris*) and the western yellow pine (*Pinus ponderosa*). Samples are plank ends. The samples (spruce, pine, and western south pine) are of ordinary, dried wood planks with ends smoothed with belt sanding machine to remove the roughness caused by the cutting process. Five pine samples, two spruce samples and two western yellow pine samples were measured.

Spectral reflectance of the tree species is studied by spectral camera (*Adimec®-1600m*). Spectral camera equipment is located at University of Joensuu, InFotonics Centre. Camera is based on PGP (prism-grating-prism) component and CCD-detector having 1600 x 500 elements. Samples are illuminated with a white light source, angle of incidence being 45°. The camera is located to the normal of the sample (45°/0° geometry). One line is imaged at the time, and the final spectral image is combination of the scanned lines. The sample is moved in steps of 0.01 that are also the spatial resolutions in vertical direction. Reflectance as a function of wavelength is measured for each pixel, i.e. vertical cells of the CCD-detector represent spatial information (pixels of the measured line) and horizontal cells wavelength distribution of the reflected light. Spectral range is from 400 nm to 1000 nm. Spectral interval of 5 nm is used in both cameras.

An example of the measured image data is provided in Fig. 1.

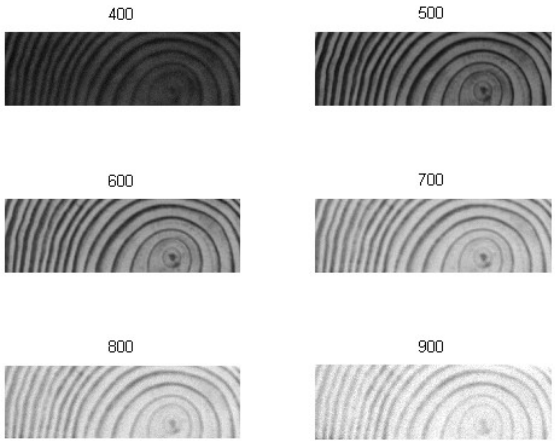

Fig. 1. Example of the western yellow pine (*Pinus ponderosa*) plank end reflectance measurement. The wavelengths are 400, 500, 600, 700, 800 and 900 nm. The gray values of the images are visually comparable. The images show a trend of higher mean reflectance in longer wavelengths. The visibility of the annual rings seems to vary between the different measurements. The image at 900 nm appears to be noisy.

4. VISIBILITY CURVE FOR ANNUAL RINGS

The main goal of the plank end spectral analysis is to find the best possible wavelengths to annual ring analysis. The spectral camera measures a series of images as a function of wavelength. This allows the use of image processing techniques to estimate the visibility of annual rings for each wavelength separately. The annual ring visibility can be estimated using several measures. The visibility can be expressed as contrast [13] of the spring wood and the summer wood mean intensities. The average contrast between the previous summer wood and the current spring wood as a function of wavelength is defined as

$$C(\lambda)=\frac{\mu_{sp}(\lambda)-\mu_{su}(\lambda)}{\mu_{su}(\lambda)}, \quad (2)$$

where $\mu_{sp}(\lambda)$ is the mean intensity of the spring wood and the $\mu_{su}(\lambda)$ is the mean intensity of the spring wood.

The contrast computation requires segmentation of the image to the summer and spring wood. This might be somewhat difficult due to the fact that there seems to be no clear border between the spring and the summer wood during the same growth season. The change of intensities is clearer between previous the summer wood and the current spring wood. Example of this is shown in Fig. 2.

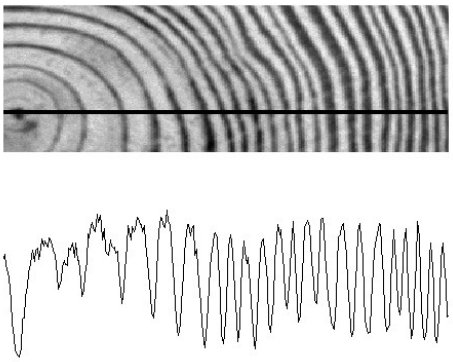

Fig. 2. The change of intensity between the summer and the spring wood. The upper part of the image shows a western yellow pine (*Pinus ponderosa*) at 500 nm. The black horizontal line shows where the intensity profile is taken. The intensity profile is shown on the lower part of the image. There is no clear border between the spring and summer wood during the same growth season. The clearest difference is between the previous summer wood and the current spring wood.

The need for the direct segmentation of the plank end is not necessary if different visibility measurements from the contrast are used. The visibility curve estimation can be based on the different variance metrics such as signal-to-noise ratio [10]. Two different metrics are used for the annual ring visibility characterization. The first metric is the standard deviation of the total signal divided with the estimated noise. The first metric is defined as

$$V_1(\lambda)=\frac{\sigma(\lambda)}{\sigma_N(\lambda)}, \quad (3)$$

where $\sigma(\lambda)$ is the standard deviation of the image and $\sigma_N(\lambda)$ is the standard deviation of the estimated noise. The noise can be estimated as in [18] or from the power spectrum using radial frequencies larger than 0.5 with whiteness assumption. Both methods should produce quite similar results.

The second visibility function is the ratio of the estimated annual ring standard deviation and the estimated background. The second visibility function is defined as

$$V_2(\lambda)=\frac{\sigma_A(\lambda)}{\sigma_B(\lambda)}, \quad (4)$$

where $\sigma_A(\lambda)$ is the standard deviation of the annual rings and $\sigma_B(\lambda)$ is the standard deviation of the background.

The estimation of the standard deviations is based on the 2-D Fourier-power spatial spectrum estimates. The spatial power spectrum density function (*psd*) describes the variance of the signal as a function of frequency after trend removal [10].

4.1. 2-D Fourier-transform and power spectrum

The spectral camera produces an image series. The image at wavelength λ are denoted as $f(o, p)$, where o and p are the positions of the pixels in the image using matrix ij-coordinate system. The 2-D signal or image $f(o, p)$ is a M x N matrix and is defined as

$$f(o,p)=\begin{bmatrix} f(1,1) & \dots & f(1,N) \\ \vdots & & \\ f(M,1) & \dots & f(M,N) \end{bmatrix}$$

The 2-D discrete Fourier-transform represents the 2-D signal as a sum of complex sinusoids. The 2-D Fourier transform as commonly known matrix notation is

$$F(u,v)=\Phi(m,m)f(o,p)\Phi(n,n), \quad (5)$$

where u and v are the frequency axes, $u = kf_x/N$, $k = 0,1, \dots, N-1$ and $v = lf_y/M$, $l = 0,1,\dots, M-1$. The $\Phi(m, m)$ and $\Phi(n, n)$ are the forward transformation kernels. The 2-D signal spatial resolutions are f_x [1/mm] and f_y [1/mm].

The J x J forward transformation matrices $\Phi(J, J)$ contain the complex sinusoids and are defined as

$$\Phi(J,J)=\frac{1}{J}\exp\left(-i\frac{2\pi}{J}kl\right), \quad (6)$$

where i is the imaginary part and $k, l = 0,1,\dots, J-1$.

The 2-D Fourier transform is rarely computed directly using matrix multiplications. Faster computational methods such as [11] are used instead.

The power spectrum estimate is the squared absolute value of the Fourier-transform. That is

$$S(u,v)=|F(u,v)|^2. \quad (7)$$

The direct power spectrum estimates are rarely used by them selves. The use of rectangular windowing causes spectral leakage. This effect and the random variation can be reduced using the Welch-estimate [5].

An example of a log end and its spatial spectrum is given in Fig 3.

4.2. Variance estimation from 2-D spectrum

The sum of the discrete 2-D spectrum over the spatial frequencies equals to the total variance of image (after removal of mean and long wave lengths). The variance of the selected spatial frequency region is estimated as the

sums of the volumes over the selected region v. The volume elements are considered to have area of $\Delta f_x \Delta f_y$ and height of $S(u, v)$. The variance at given spatial frequencies (q, w) is

$$P = \Delta f_x \Delta f_y \sum_{q \in v} \sum_{w \in v} S(q, w)$$

where Δf_x and Δf_y are the frequency resolutions of the frequency axes in x- and y- directions. The estimate of the frequency resolution in x-direction are defined for the Welch estimate as

$$\Delta f_x = \frac{f_x}{n}.$$

The selected regions are circular in the spectral domain thus selecting a region that has constant radial frequency. The minimum and maximum radial frequencies are selected based on the annual ring widths. An example of the selected spatial frequency domain is shown in Fig. 4.

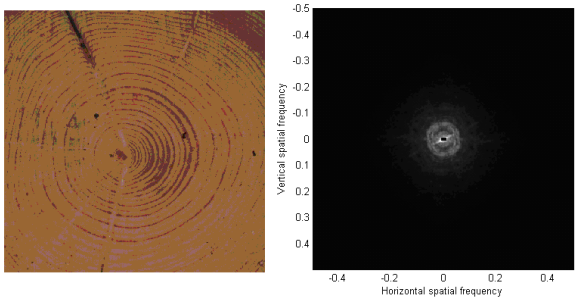

Fig. 3. An example of the log end and its spatial power spectrum. The upper part of the image shows a pine (*Pinus sylvestris*). The computed spatial power spectrum is shown on the lower part of the image. The areas having the most variance are shown as brighter colour. The bright disk or circular like structure in the centre of the spectrum is caused by the annual rings.

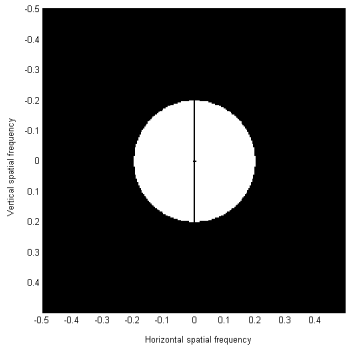

Fig. 4. An example of the spatial domain used for the visibility curve estimation. The white areas are used for the variance estimation. The dark vertical line is left out of the computation due to removal of scanning artefacts.

5. RESULTS OF THE REFLECTANCE AND VISIBILITY CURVE COMPUTATION

The resulting mean curves are shown for pine (*Pinus sylvestris*), spruce (*Picea abies*) and for western yellow pine (*Pinus ponderosa*) in Fig. 5, Fig. 6, and Fig. 7, respectively.

The resulting visibility curves from the first method for the pine, the spruce and the western yellow pine are shown in Fig 8., Fig 9., and Fig 10., respectively. The visibility curves visibility curves from the second method for the pine, the spruce and the western yellow pine are shown in Fig 11., Fig 12., and Fig 13., respectively.

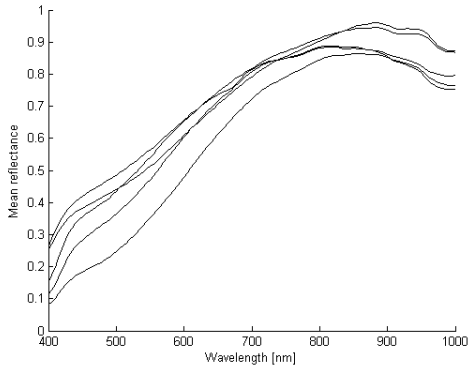

Fig. 5. The mean reflectance curves for five pine (*Pinus sylvestris*) samples.

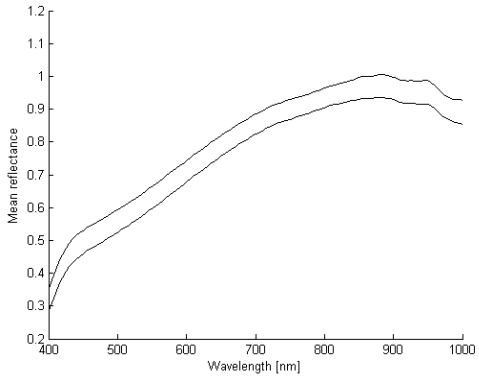

Fig. 6. The mean reflectance curves for two spruce (*Picea abies*) samples.

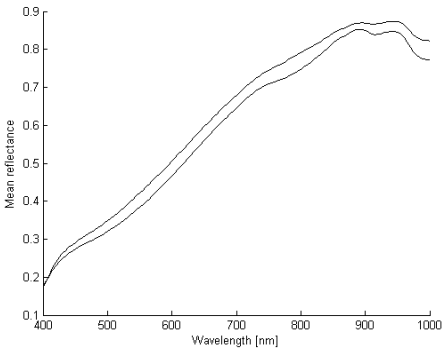

Fig. 7. The mean reflectance curves for two western yellow pine (*Pinus ponderosa*) samples.

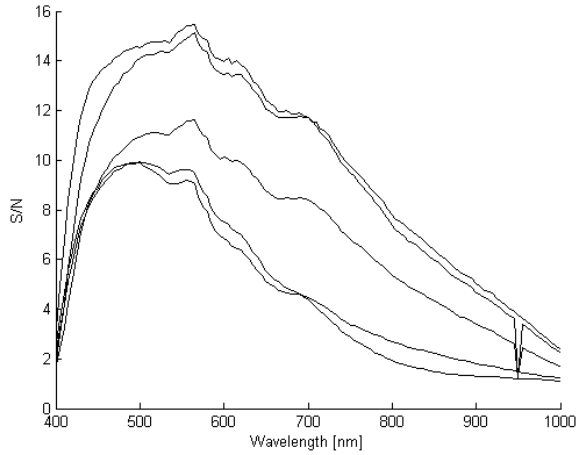

Fig. 8. The visibility curves for five pine (*Pinus sylvestris*) samples using (3). The downwards peak at approximately 950 nm is probably produced by the measurement device.

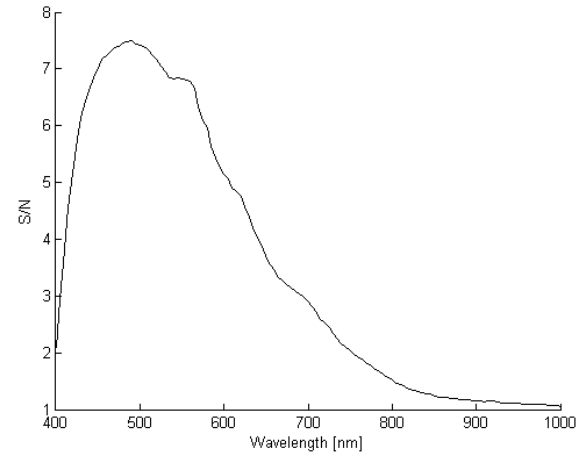

Fig. 9. The visibility curves for two spruce (*Picea abies*) samples using (3).

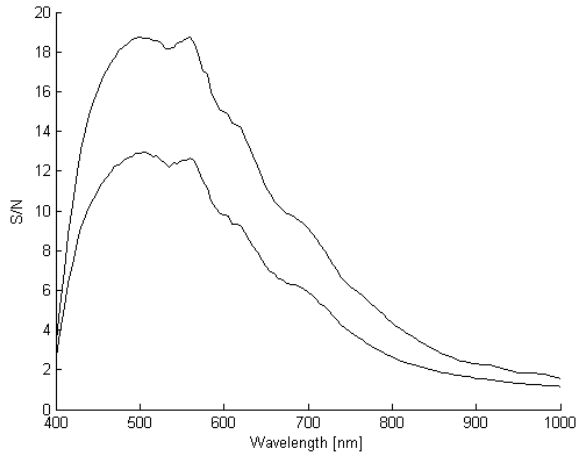

Fig. 10. The visibility curves for two western yellow pine (*Pinus ponderosa*) samples using (3).

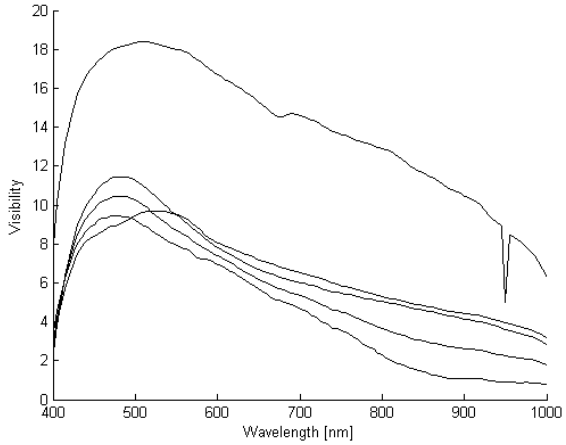

Fig. 11. The visibility curves for five pine (*Pinus sylvestris*) samples using (4). The downwards peak at approximately 950 nm is probably produced by the measurement device.

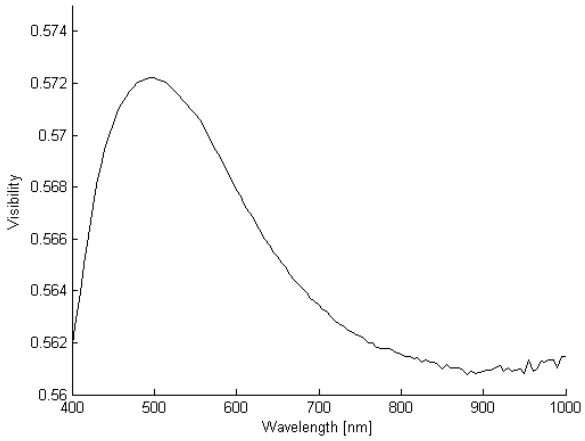

Fig. 12. The visibility curves for two pine (*Picea abies*) samples using (4).

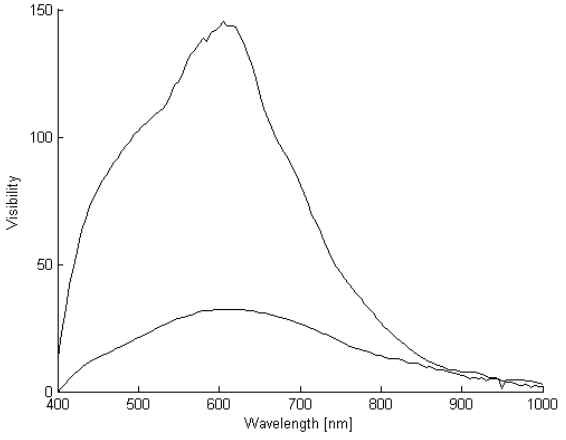

Fig. 13. The visibility curves for two western yellow pine (*Pinus ponderosa*) samples using (3). The level of visibility metrics are of different level.

5. CONCLUSION

The mean reflectance curves rise from 400 nm to approximately 800 nm. The maxima are shown in longer wavelengths from 800 nm to 950 nm. The first visibility method curve shows that the maximum visibility for annual rings is obtained between 500-650 nm. The second visibility method shows somewhat smaller wavelengths between for the tree species selected. This seems to imply that the annual rings are more clearly detected at these wavelengths and are not connected directly to the mean reflectance curve. The results are computed only for the three coniferous tree species. The results are might be applicable to other coniferous trees encountered on the northern hemisphere. The results are expected to provide different results for the deciduous trees.

The analysis methods provide estimates of the annual ring visibility without a prior segmentation of the rings. The methods provide quite similar results except for the western yellow pine. The position of the maximum visibility is shifted to longer wavelengths. The results provided by the first metric seem to be more reliable when contrast is computed by selecting points manually.

The reliability of the results depends on the number of samples, on the selection of samples, on the handling of the samples and on the analysis methods. The measuring device and analysis algorithms add their contribution to the uncertainty. The number of samples is quite small for further statistical analysis. Fortunately, the results for different samples seem to have similar characteristics.

The selection and handling of the samples contain several possibilities that affect the results. The sample selection contains a choice between fresh and dried wood. The selected samples are of dried wood. The selected samples had some knots, but these areas are left out of the analysis. The samples are smoothed before measurement. The sample surface smoothing is the main factor in sample handling. The smoothing is done quite similarly to all the samples to provide minimum uncertainty caused by the sample surface roughness.

The visibility curves show that the optical design of the lighting and the optical filtering is suitable for the silicon based sensors having best quantum efficiencies approximately in that region. The visibility curves for the deciduous trees have to be measured before the whole system can be designed.

ACKNOWLEDGMENTS

Thanks to Jouni Hiltunen (PhD, Laboratory Engineer), University of Joensuu / InFotonics Center for instructions and assistance in using of the spectral camera equipment.

REFERENCES

[1] H. Kauppinen, O. Silvén. “The Effect of Illumination Variations on Color-Based Wood Defect Classification”. Proceedings of the 1996 International Conference on Pattern Recognition (ICPR '96) Volume III-Volume 7276 - Volume 7276, pp. 828-832. 1996.

[2] C. D'Andrea, A. Farina, D. Comelli, A. Pifferi, P. Taroni, G. Valentini, R. Cubeddu, L. Zoia, M. Orlandi, and A. Kienle, "Wood Characterization by Diffuse Time-Resolved Optical Spectroscopy," in *Laser Applications to Chemical, Security and Environmental Analysis*, OSA Technical Digest (CD) (Optical Society of America, 2008), paper LTuC5.

[3] K. Marjanen, P. Ojala, H. Ihalainen. “Measurements of annual ring width of log ends in forest machinery”, SPIE, (Conference Proceedings Paper) vol. 6812, March 2008.

[4] Bishop C.M. *Pattern recognition and machine learning*, pp.561, Springer, New York, 2006.

[5] Welch, P.D, "The Use of Fast Fourier Transform for the Estimation of Power Spectra: A Method Based on Time Averaging Over Short, Modified Periodograms", *IEEE Transactions Audio Electroacoustics*, Vol. AU-15, June 1967, pp.70-73.

[6] H. Kauhanen, "Close range photogrammetry –structured light approach for machine vision aided harvesting”, T*he international Archives of Photogrammetry, Remote Sensing and Spatial Information Sciences*, vol. XXXVIII, part B5, 2008, pp. 75-80.

[7] E. M. Mikhail, J. S. Bethel, J. C. McGlone, *Introduction to modern photogrammetry,* John Wiley and sons, inc., 2001.

[8] N. S. Kopeika, *A system engineering approach to imaging*, SPIE , 1998.

[9] T. Hanning, R. Kickingereder, D. Casacent, "Determining the average annual ring width on the front side of lumber", *Proceedings of SPIE*, vol. 5144, SPIE 2003, pp. 707-716.

[10] O. Aumala, H. Ihalainen, H. Jokinen, J. Kortelainen, *Mittaussignaalien käsittely*, 2. edn, Pressus Oy, Tampere, 1995.

[11] M. Frigo, S. G. Johnson, "The design and implementation of FFTW3", *Proceedings of IEEE*, vol. 93, no. 2, IEEE 2005. pp. 216-231.

[12] E. L. Dereniak, G. D. Boreman, *Infrared detectors and systems*, John Wiley and sons, inc., 1996.

[13] B. Chanda, D. D. Majumder, *Digital image processing and analysis*, Prentice-Hall of India Private Limited, 2005.

[14] I. C. G. Vieira, A. S. de Almeida, E. A. Davidson, T. A. Stone, C. J. R. de Carvalho, J. B. Guerrero, "Classifying successional forests using Landsat spectral properties and ecological characteristics in eastern Amazônia", *Remote Sensing of Environment*, no. 87, Elsevier 2003, pp. 470-481.

[15] D. M. Gates, H. J. Keegan, J. C. Schleter, V. R. Weidner, "Spectral properties of plants", *Applied Optics*, vol. 4, iss. 1, OSA, 1965, pp. 11-20.

[16] T. M. Lillesand, R. W. Kiefer, *Remote sensing and image interpretation*, John Wiley and sons, inc., 2000.

[17] T. Key, T, A. Warner, J. B. McGraw, M. A. Fajvan, "A comparison of multispectral information on high spatial resolution imagery for classification of individual tree species in an temperate hardwood forest", *Remote Sensing of Environment*, vol. 75, no. 1, Elsevier 2001, pp. 100-112.

[18] K. Marjanen, O. Yli-Harja, "Analysis of system noise in thermal imagers", P*roceedings of SPIE*, vol. 5017, SPIE 2003, pp. 228-239.